

## Nonlinear Perturbation Theory of the Incompressible Richtmyer-Meshkov Instability

Alexander L. Velikovich

*Berkeley Scholars, Inc., Springfield, Virginia 22150*

Guy Dimonte

*Lawrence Livermore National Laboratory, Livermore, California 94551*

(Received 11 January 1996)

A single-mode nonlinear high-order perturbation theory is developed to describe the Richtmyer-Meshkov instability of an impulsively accelerated interface between an incompressible fluid and a constant supporting pressure. The nonlinear modification of Richtmyer's formula is presented and compared to experimental data with strong radiatively driven shocks. The theory allows a straightforward extension to more general cases of Richtmyer-Meshkov and Rayleigh-Taylor instabilities (multimode, more interfaces, three-dimensional flow, etc.). [S0031-9007(96)00038-5]

PACS numbers: 47.20.Ma, 47.40.Nm

The Richtmyer-Meshkov (RM) instability develops when a plane shock wave interacts with a corrugated contact interface between two different fluids [1,2]. Like the Rayleigh-Taylor (RT) instability, the RM instability is important in a wide range of applications, from astrophysics to inertial confinement fusion. Both numerical [3] and analytical [4–6] methods developed in recent years are available to calculate the linear growth rate of the RM instability.

The nonlinear theory of the RM instability, as distinct from numerical studies, is being developed under the simplifying assumption of incompressibility. Still, its main results are based on simplified models of incompressible flow (see Ref. [7] and references therein). Exact perturbation theory has been advanced mostly for the RT instability. Ingraham [8] proposed a method for calculating arbitrarily high orders of the perturbation series, and actually carried out the solution to second order in the perturbation parameter  $\epsilon$ . Perturbation theory was later developed to third order in a 3D problem [9]. For the incompressible RM instability, only two conflicting estimates of the second-order term have been published so far: In Ref. [10], this term is predicted to be identically zero, whereas in Refs. [11] and [12] a nonzero term is obtained.

Note that the real power of perturbation theory is not revealed as long as we are limited to a few high-order terms because the convergence of the perturbation series in the expansion parameter  $\epsilon$  is unclear. To ascertain the convergence, the expansion must include a large number of terms. So far, the calculation of higher-order terms has been perceived as a serious problem, whose complexity escalates with increased order.

The goal of this work is to attract attention to the following remarkable fact. With symbolic computation software, the calculation of the higher-order terms is no longer a serious problem. Terms of all orders are readily generated by a simple procedure based on Ingraham's work [8]. The maximum order is limited only by the

available computing power. Although in the present Letter we treat the most simple case of the RM instability with Atwood number  $A = 1$ , all the above is true not only for arbitrary Atwood number but for a very large number of nonlinear instability problems, including all the relevant RT problems—interface, finite fluid layer, combination of fluid layers, single or multimode, with or without surface tension, 2D or 3D.

The problem studied here is formulated as follows (for details, see Refs. [1,7,8]). An incompressible fluid supported by constant pressure occupies the upper half space bounded by the interface  $y = \eta(x, t)$ . Initially, the fluid is at rest, and the interface has a cosine shape,  $\eta(x, t < 0) = \eta_0 \cos kx$ . The motion is excited by a gravity acceleration pulse  $g(t) = U\delta(t)$ . Our units of length and time are  $k^{-1}$  and  $(kU)^{-1}$ , respectively. We normalize the interface displacement to  $\eta_0$ , introducing  $\xi(x, t) = \eta(x, t)/\eta_0$ , and the velocity potential to  $\eta_0 U$ . The perturbation parameter is defined as  $\epsilon = k\eta_0$ . The flow is described by Bernoulli's equation

$$\xi \delta(t) + \frac{\partial \phi}{\partial t} + \frac{1}{2} \epsilon (\nabla \phi)^2 = 0 \quad (1)$$

and by the kinematic condition

$$\frac{\partial \xi}{\partial t} = \frac{\partial \phi}{\partial y} - \epsilon \frac{\partial \phi}{\partial x} \frac{\partial \xi}{\partial x}. \quad (2)$$

Equations (1) and (2) should be satisfied at the interface,  $y = \epsilon \xi(x, t)$ . The velocity potential  $\phi(x, y, t)$  is a harmonic function:  $\nabla^2 \phi = 0$ .

For  $t > 0$ , the acceleration term in Eq. (1) is zero. To relate the strength of the impulsive force to the subsequent fluid motion, we integrate Eq. (1) from  $t = -0$  to  $t = +0$  (below,  $t = 0$  always means  $t = +0$ ) and obtain the initial conditions

$$\cos x + \phi(x, \epsilon \cos x, 0) = 0, \quad \xi(x, 0) = \cos x. \quad (3)$$

We seek a solution of Eqs. (1) and (2) with the initial conditions (3) as formal power series in  $\epsilon$ :

$$\xi(x, t) = \sum_{j=0}^{\infty} \epsilon^j \xi_j(x, t), \quad \phi(x, y, t) = \sum_{j=0}^{\infty} \epsilon^j \phi_j(x, y, t). \tag{4}$$

The method of solution will be described separately, but the idea is simple: Make the computer follow Ingraham's procedure [8]. Here are some of the results:

$$\begin{aligned} \xi_2(x, t) &= \left(\frac{3}{8}t^3 - \frac{3}{8}t^2\right)\cos 3x - \left(\frac{5}{24}t^3 + \frac{1}{8}t^2 + \frac{1}{4}t\right)\cos x, \\ \xi_3(x, t) &= \left(-\frac{1}{3}t^4 + \frac{2}{3}t^3 - \frac{1}{4}t^2\right)\cos 4x + \left(\frac{1}{3}t^4 + \frac{1}{2}t^2 + \frac{1}{12}t\right)\cos 2x, \dots \\ \xi_n(x, t) &= \left[(-1)^n \frac{(n+1)^{n-1}}{2^n n!} t^{n+1} + O(t^n)\right]\cos[(n+1)x] + \dots \end{aligned} \tag{6}$$

The analytic formula (6) has been obtained by inspection, not derived rigorously. Still, since its validity has been checked for the first 20 orders, there is a good chance that it is true for higher orders also.

Calculation of the higher-order terms is only a starting point of the perturbation theory analysis. Its main issues are convergence and analytic continuation. Below, we address these issues only for  $t = 0$  and  $\epsilon \rightarrow 0$ , which physically corresponds to nonlinear modification of Richtmyer's formula and to the study of evolution of initially small perturbations, respectively.

In Ingraham's RT case [8], at  $t = 0$  the fluid remains at rest, and convergence of his perturbation series is trivial. Here, at  $t = 0$  the fluid has already been set into motion by the acceleration pulse. The growth rates  $\Gamma = \partial \xi / \partial t$  at  $t = 0$  predicted by the linear Richtmyer's formula (5) for the bubble ( $x = 0$ ) and the spike ( $x = \pi$ ) are  $\pm 1$  or, in dimensional form,  $\pm kU \eta_0$ . Nonlinear theory adds higher-order corrections to this formula:

$$\Gamma_b(t = 0, \epsilon) = 1 - \frac{1}{4}\epsilon^2 + \frac{1}{12}\epsilon^3 + \frac{19}{192}\epsilon^4 - \frac{21}{320}\epsilon^5 - \frac{461}{11520}\epsilon^6 + \frac{347}{8064}\epsilon^7 + \dots, \tag{7}$$

$$\Gamma_s(t = 0, \epsilon) = -\Gamma_b(t = 0, -\epsilon). \tag{8}$$

The radius of convergence of the series (7) is found to be close to  $|\epsilon| = 1$ , hence the series generates an analytic function of  $\epsilon$  in the vicinity of  $\epsilon = 0$ . As demonstrated by Eq. (8), the growth rates for both cases are given by the same analytic function of complex  $\epsilon$ , which has at least one singularity on the circle of convergence. If the singularities are not located on the real axis, then this function could be continued analytically along it to higher values of  $|\epsilon| > 1$ . The conventional technique for doing this is the use of Padé approximation [12–14].

Figure 1 shows the nonlinear modification of Richtmyer's formula. The growth rates obtained for the bubble,

$$\xi_0(x, t) = (t + 1) \cos x \tag{5}$$

(this is the well-known linear Richtmyer's formula),

$$\xi_1(x, t) = -\frac{1}{2}t^2 \cos 2x$$

(this term is the same as given in Refs. [11] and [12], and not as given in Ref. [10]),

the spike, and the average value,  $\Gamma_{av} = (\Gamma_b - \Gamma_s)/2$ , which is typically measured in the experiments, are normalized with respect to the results of the linear theory. Here, three Padé approximants to the series (7),  $P_{10}^{10}$ ,  $P_{12}^{12}$ , and  $P_{16}^{16}$  (the corresponding orders of approximation are 21 to 33), are shown versus positive  $\epsilon$ . Partial sums of the series (7) follow the same curves up to  $\epsilon = 1$ , and then rapidly diverge. Poles of the Padé approximants indicate the singularities limiting the radius of convergence: They are located at  $\epsilon = \pm i$  and are probably branch points. Other poles are located in the  $\text{Re} \epsilon < 0$  half plane, which explains slower convergence of the Padé approximants for the spike growth rate.

The points are from RM experiments [15] with strong radiatively driven shocks on the Nova laser at Lawrence Livermore National Laboratory. The shock is initiated

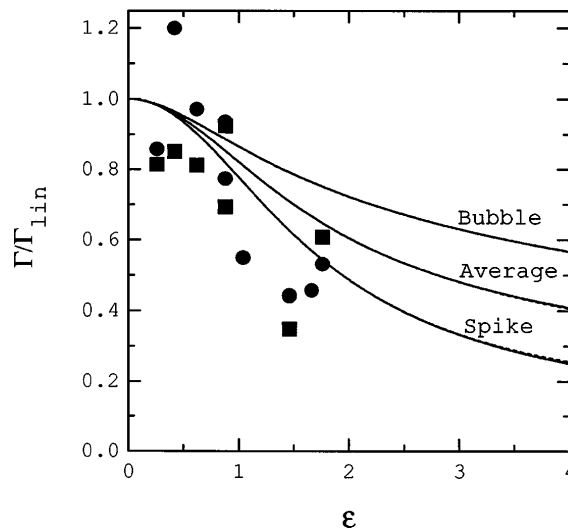


FIG. 1. Nonlinear modification of Richtmyer's formula for instantaneously gained growth rate  $\Gamma$  vs  $\epsilon$ . Dotted, dashed, and solid lines are Padé approximants  $P_{10}^{10}$ ,  $P_{12}^{12}$ , and  $P_{16}^{16}$ , respectively. Points are the measured average growth rates normalized with the rates given by compressible linear theory.

in a beryllium (Be) ablator ( $1.7 \text{ g/cm}^3$ ) and is transmitted into a foam tamper ( $0.12 \text{ g/cm}^3$ ). A sinusoidal perturbation  $\eta_0 \sin kx$  is imposed at the Be/foam interface with  $4 \leq \eta_0 \leq 14 \text{ } \mu\text{m}$  and  $30 \leq 2\pi/k \leq 150 \text{ } \mu\text{m}$ . The RM growth rate (averaged over bubbles and spikes) is measured with face-on and side-on radiography using x-ray dopants in the foam. Since the experiments have  $A = -0.87$  and high compression (Mach  $> 10$ ), we normalize the measured growth rates to those calculated with the analytical linear theory [6], which is valid only when  $k\eta_0 \ll 1$  (the nonlinear correction factor  $\Gamma_{av}/\Gamma_{lin}$  is almost independent of the Atwood number). The circles

and boxes correspond to 30 and 15 Mbar shock drive pressures, respectively. As can be seen, the points agree within the experimental scatter with the calculated nonlinear correction averaged for the bubbles and spikes.

Substituting the coefficients  $\xi_j(x, t)$  into the expansion (4) for  $\xi$ , we note that the result could be regarded also as a Taylor series in time. To make it meaningful, we normalize the time variable. The linear growth rate is proportional to the initial amplitude  $\eta_0$ , that is, to  $\epsilon$ , hence the time interval needed to reach the nonlinear regime is of the order of  $1/\epsilon$ . Introducing  $\tau = \epsilon t$ , we obtain the series sought for. In particular,

$$\eta_b(\tau, \epsilon) = \tau - \frac{1}{2} \tau^2 + \frac{1}{6} \tau^3 - \frac{7}{120} \tau^5 + \frac{1}{12} \tau^6 - \frac{341}{5040} \tau^7 + \frac{37}{1680} \tau^8 + \dots$$

$$+ \epsilon \left( 1 - \frac{1}{2} \tau^2 + \frac{2}{3} \tau^3 - \frac{3}{8} \tau^4 - \dots \right) + \epsilon^2 \left( -\frac{1}{4} \tau + \frac{1}{4} \tau^2 + \frac{3}{8} \tau^3 - \frac{47}{48} \tau^4 + \dots \right) + \dots, \quad (9)$$

$$\eta_s(\tau, \epsilon) = \eta_b(-\tau, -\epsilon), \quad (10)$$

for the bubble and the spike, respectively.

Passing to the limit  $\epsilon \rightarrow 0, t \rightarrow \infty$ , finite  $\tau$ , and retaining only the zero-order terms in  $\epsilon$ , we can describe evolution of an initially small perturbation to the nonlinear stage. Figure 2 shows the bubble-spike structure evolving at the interface. (For each  $x$ , the time dependence is calculated as the  $P_{10}^{10}$  Padé approximant of the zero-order series.) The spike becomes noticeably sharper than the bubble, as the structure is traced up to  $k\eta = 0.5$  and 1 (with  $\eta$  in conventional units) for the bubble and spike, respectively. Why not longer?

The reason for it is illustrated in Fig. 3, where the growth rates for the bubble and the spike given by the Padé approximants  $P_8^8, P_9^9$ , and  $P_{10}^{10}$  are presented versus  $\tau$ . For the bubble, convergence is good, and the growth rate decreases monotonically, in qualitative agreement with Refs. [7,16,17]. Since in this limit  $\eta_s(\tau) = \eta_b(-\tau)$

[see Eq. (10)], the function  $\eta_s(\tau)$  must be singular; e.g., if  $\eta_b(\tau)$  behaves as  $\ln(\tau)$  for large  $\tau$ , then  $\eta_s(\tau)$  should have a logarithmic singularity at finite  $\tau$ . Indeed, for the spike, Fig. 3 demonstrates that convergence is not improved by increasing the order of Padé approximation for  $\tau$  slightly over 0.7, which is clear signature of a singularity.

Performing partial summation of the leading terms given by Eq. (6) or of other partial sums which could be identified analytically, we generate analytic functions of  $\tau$  whose radii of convergence, all equal to  $2/e = 0.736$  (in good agreement with Fig. 3), are determined by a cut along the negative real axis from  $-\infty$  to  $-2/e$ . Not surprisingly, this resembles the analytic solution for the free-surface single-mode RT instability presented in Ref. [18], where an infinitely long spike is produced at finite time. In both cases, we have the bubble-spike symmetry  $\tau \leftrightarrow -\tau$ . This similarity indicates that the

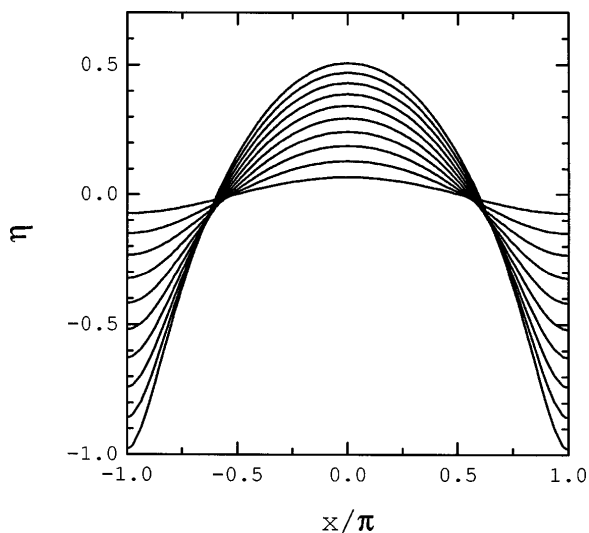


FIG. 2. Displacement of the interface in units of  $k^{-1}$  for  $\tau = 0.07, 0.14, \dots, 0.7$ .

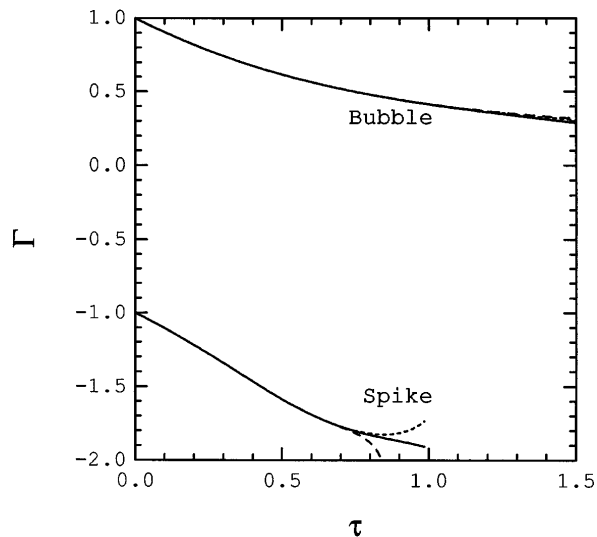


FIG. 3. Growth rate  $\Gamma$  vs time: Dotted, dashed, and solid lines are time derivatives of Padé approximants  $P_8^8, P_9^9$ , and  $P_{10}^{10}$ , respectively.

spike singularity in our case should also be logarithmic [18], which, in turn, supports the conclusion of Ref. [7] that the bubble growth at large time is logarithmic also.

What is the physical meaning of this solution after the spike singularity has been formed? Could we use it to describe the bubble or the vicinity of the spike? How would this type of singular behavior be modified in the case of arbitrary Atwood number, where mushrooming is expected? Could the branching of an analytic function of complex  $\tau$  adequately describe the multivalued solution at the mushrooming stage? These are some of the questions to be answered by the perturbation theory analysis. The answers are beyond the scope of the present Letter.

Useful discussions with D. Book, V. Krasnopolsky, and M. Schneider are acknowledged with gratitude. Special thanks are due to Stephen Bodner for his support and encouragement. This research was supported by the U.S. Department of Energy through a contract for the Naval Research Laboratory, and the experiment was performed under Contract No. W-7405-ENG-48.

---

[1] R. D. Richtmyer, *Commun. Pure Appl. Math.* **13**, 297 (1960).

- [2] E. E. Meshkov, *Fluid Dyn.* **4**(5), 101 (1969).  
[3] Y. Yang, Q. Zhang, and D. H. Sharp, *Phys. Fluids* **6**, 1856 (1994).  
[4] G. Fraley, *Phys. Fluids* **29**, 376 (1986).  
[5] A. L. Velikovich, L. Phillips, and J. Dahlburg (to be published).  
[6] A. L. Velikovich, *Phys. Fluids* (to be published).  
[7] J. Hecht, U. Alon, and D. Shvarts, *Phys. Fluids* **6**, 4019 (1994).  
[8] R. L. Ingraham, *Proc. Phys. Soc., Sect. B* **67**, 748 (1954).  
[9] J. W. Jacobs and I. Catton, *J. Fluid Mech.* **187**, 329 (1988).  
[10] K. O. Mikaelian, *Phys. Rev. Lett.* **73**, 3177 (1994).  
[11] S. W. Haan, *Phys. Fluids B* **3**, 2349 (1991).  
[12] Q. Zhang and S.-I. Sohn, *Phys. Lett. A* **212**, 149 (1996).  
[13] C. M. Bender and S. A. Orszag, *Advanced Mathematical Methods for Scientists and Engineers* (McGraw-Hill, New York, 1978).  
[14] G. A. Baker and P. Graves-Morris, *Padé Approximants* (Addison-Wesley, Reading, MA, 1981).  
[15] G. Dimonte *et al.*, *Phys. Plasmas* **3**, 614 (1996).  
[16] U. Alon *et al.*, *Phys. Rev. Lett.* **74**, 534 (1995).  
[17] J. W. Grove, R. H. Holmes, and D. Sharp, *J. Fluid Mech.* **30**, 51 (1995).  
[18] J. K. Dienes, *Phys. Fluids* **21**, 736 (1978).